SIMULATION OF THE OPTICAL PROPERTIES OF ATMOSPHERIC AEROSOLS IN THE PLANETARY BOUNDARY LAYER

Final Technical Report
by

Rosalba Saija
(September 2002)

United States Army

EUROPEAN RESEARCH OFFICE OF THE U.S. ARMY

London, England

CONTRACT NUMBER N68171-01-M-5907

Contractor: Prof. Gaetano Silvestri

Università di Messina, Dipartimento di Fisica della Materia e Tecnologie Fisiche Avanzate

Salita Sperone 31 – Messina 98166 - Italy

The Research reported in this document has been made possible through the support and sponsorship of the US Government through its European Research Office of the U.S. Army. This report is intended only for the internal management use of the contractor and of U.S. Government.

20030910 08

REPORT DOCUMENTATION PAGE

Form Approved
OMB No. 0704-0188

maintaining the data needed, and completing and reviewing this collection of information. Send comments regarding this burden estimate or any other aspect of this collection of information, including suggestions for reducing this burden to Washington Headquarters Services, Directorate for Information Operations and Reports, 1215 Jefferson Davis Highway, Suite 1204, Arlington, VA 22202-4302, and to the Office of Management and Budget, Paperwork Reduction Project (0704-0188), Washington, DC 20503

1. AGENCY USE ONLY (Leave blank)	2. REPORT DATE	3. REPORT TYPE AND DATES COVERED
	25 September 2002	Final Technical Report 09/08/2001-09/08/2002

4. TITLE AND SUBTITLE
Simulation of the Optical Properties of Atmospheric Aerosols in the Planetary Boundary Layer (PBL)

5. FUNDING NUMBERS
9199-EN-01
N68171-01-M-5907

6. AUTHOR(S)
Dr Rosalba Saija

7. PERFORMING ORGANIZATION NAME(S) AND ADDRESS(ES)
University of Messina
Dept. "Fisica della Materia e TFA"
Salita Sperone 31
98166 Messina - ITALY

8. PERFORMING ORGANIZATION REPORT NUMBER

9. SPONSORING / MONITORING AGENCY NAME(S) AND ADDRESS(ES)
US Army – European Research Office
Edison House,
223 Old Marylebone Road
London NW1 5TH
United Kingdom

10. SPONSORING / MONITORING AGENCY REPORT NUMBER

11. SUPPLEMENTARY NOTES

12a. DISTRIBUTION / AVAILABILITY STATEMENT
PUBLIC RELEASE

12b. DISTRIBUTION CODE

13. ABSTRACT ***(Maximum 200 Words)***

We report in this paper the relevant results obtained for the calculation and the retrieving of the optical properties of the particles that can constitute the atmospheric aerosols.

In the first section we present the preliminary results of computations of the optical properties (extinction and backscattering) for low density dispersions of particles with an irregular shape. These particles are modelled as clusters of spheres and the calculated Lidar ratios will be compared with the other computations performed using spheres with Mie theory. The values of the lidar ratio will also constitute the data base for the interpretation of the experimental data obtained with LIDAR systems.

In the second section we implemented a neural network that proved to be a useful tool for the recognition of the microphysical properties of a low density dispersion of spherical particles from the angular pattern. In future we plan to extend the algorithm to the recognition of the optical parameters for nonspherical particles.

In the third section we have explored the scattering properties of the irregular shaped aerosols by means an angular analysis in the IR-VIS range aimed to compare the calculated scattering patterns with the experimental ones obtained with a two-dimensional angular optical scattering device (TAOS). More extended comments are contained in a paper that will be published in Applied Optics.

14. SUBJECT TERMS
Optical Properties – Electromagnetic Scattering – Lidar – Recognition Pattern
Atmospheric Aerosols

15. NUMBER OF PAGES
21

16. PRICE CODE

17. SECURITY CLASSIFICATION OF REPORT	18. SECURITY CLASSIFICATION OF THIS PAGE	19. SECURITY CLASSIFICATION OF ABSTRACT	20. LIMITATION OF ABSTRACT
Unclassified	Unclassified	Unclassified	UL

relatively large particles, it can be driven across the Atlantic Ocean until the south, central and north part of America.

- Optical Parameters

The desert dust is composed by highly irregular shaped particles that cannot be described as spheres. Our technique is able to describe these particles as clusters of spheres, possibly characterized by different refractive indices, whose arrangement is chosen so as to simulate, as best as possible, the real components of the aerosols. This approach offers many advantages: it allows us both to determine the correct scattering pattern that, even after the random averaging procedure over the orientations is performed, still resembles the asymmetry of the constituent objects(1,2); both to follow the change in the optical properties when, due to natural processes, the single scatterer changes its morphology (3,4). Furthermore, the T-matrix approach enables us to determine analytically, when necessarily, averages over non-random orientational distributions, once an appropriate weight function is introduced (5,6).

To simulate the configurationally anisotropy, we choose different cluster models composed of 4 or 5 spheres arranged as in Fig. a.

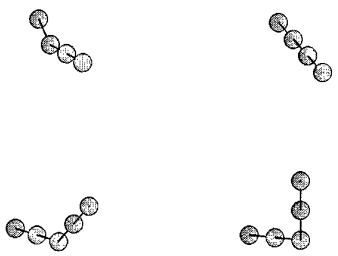

Fig. (a)

At λ=351 nm we used for the refractive index *n=1.5225+i0.006.*

- Size distributions

The desert dust ranges over several orders of magnitude in size from 10^{-2} μm to 10^{2} μm. The observations suggest a size distribution represented by means of a trimodal lognormal function; however the third mode that has a modal radius of 5 μm can be neglected as it represents a size distribution of particles that have a great settling rate. For this reason we consider a bimodal lognormal distribution with the following expression

$$\frac{dN_i(r)}{d\log r} = \frac{N_i}{\sqrt{2\pi}\log\sigma_i}\exp\left(-\frac{(\log r - \log r_i)^2}{2(\log\sigma_i)^2}\right) \quad i=1,2$$

In this formulation N_i is the total number of particles per unit volume, r_i and σ_i the distribution of the geometric radius and width, respectively. The parameters we use for the distribution are derived from literature (Table 2). By varing the distribution parameters in a random way, we compute 5000 bimodal distribution that we use to perform the integral necessary to compute all the possibly a and b values for our model. In fig (b) we show some of the distributions calculated with three sets of the parameters (r_1, σ_1, N_1) and (r_2, σ_2, N_2) chosen in a random way in the range indicated in table 2.

Table 2. Parameters for the size distribution of the desert dust as reported by different authors.

r_1 (μm)	σ_1	$N_1(cm^{-3})$	r_2 (μm)	σ_2	$N_2(cm^{-3})$
0.02	1.5	180	0.3	1.5	4
0.08	1.8	1470	1.5	2.0	105

- Results and Discussion

The simulation that is still in progress, considers aerosol scatterers modelled as cluster of identical spheres whose radia are chosen so that the radius of the sphere surrounding the whole cluster ranges from 0.02 μm to 2 μm, even if, with the acquisition of more powerful computers, we plan to extend the range up to 5 μm

We present here the preliminary results obtained for the first cluster shown in fig (a).

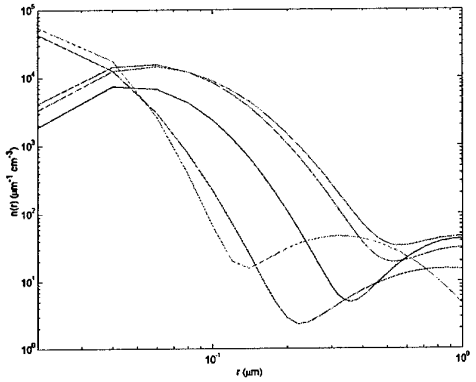

Fig (b)

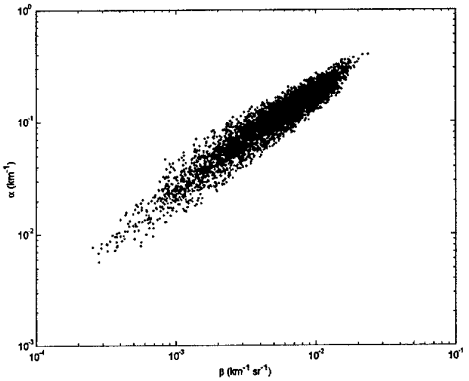

Fig (c)

In fig. (c) we report the scatterplot in a loglog scale of the extinction coefficient vs the backscattering coefficient obtained for the desert aerosol. It can be observed that we obtain a dispersion of the values that we are going to compare with the simulation that consider spherical scatterers. At a first exam these values present a more large dispersion; feature that seems to be an interesting peculiarity of the model with which it would be possible to analyze more correctly the scattered light generated by the interaction of the Lidar radiation with the atmospheric constituents.

1)F. Borghese, P. Denti, R. Saija, G. Toscano and O. I. Sindoni,Macroscopic optical constants of a cloud of randomly oriented nonspherical scatterers, Nuovo Cim. B 81, 29-50 (1984).

2)O. I. Sindoni, F. Borghese, P. Denti, R. Saija and G. Toscano, Theoretically computed optical constants and scattering properties of non-spherical scatterers, in Aerosols Liu, Pui, Fissan, eds., (Elsevier, New York1984), 810.

3) R. Saija, G. Toscano, O.I. Sindoni, P. Denti and F. Borghese, Effect of the chemical reactions on the macroscopic optical constants of a model aerosol, in Aerosols Liu, Pui, Fissan, eds. (Elsevier, New York, 1984), 817.

4)R. Saija, G. Toscano, O. I. Sindoni, F. Borghese and P. Denti, Effect of the ``chemical reactions" on the absorption coefficient of a polydisperse model aerosol, Nuovo Cim . B 85, 79-93 (1985).

5)F. Borghese, P. Denti, M.A. Iatì, R. Saija, Backscattering from model atmospheric ice microcrystals, Nuclear and Cond. Matter Phys. CP513, 43(2000)

6)F.Borghese, P. Denti, R. Saija, M.A. Iatì, O.I. Sindoni, Optical properties of a dispersion of anisotropic particles with non-randomly distributed orientations. The case of atmospheric ice microcrystals,In press in J. Quant. Spectr. & R.F. (2001).

Neural network scheme for the retrieval of size and index of refraction of microparticles from the angular scattering pattern.

The retrieval of the structure of the atmospheric constituents from experimental data is one of the most interesting problems that have been faced in these last years. As the most recent instruments are able to sample the atmosphere giving a large amount of information whose inversion require high performance computers, has grown in recent years the necessity to develop new retrieval algorithms that would not rely on detailed knowledge of physical processes involved and fast enough to be implemented in computers with low-cost hardware. Because neural networks generally exhibit these properties, we implemented this algorithm to retrieve the size and the index of refraction of a dispersion of spherical microparticles from the one angular scattering pattern.

In the framework of the neural network a scattering problem can be considered as follows: the intensity of the scattered light measured at an angle ϑ coming from a single particle embedded in an external medium, is a function of r and m, the radius and the refraction index of the particle respectively

$$I(\vartheta)=F(\vartheta,r,n)$$

Given a vector **x** containing n measured values of I for n different ϑ angles (these represent the input data), the inverse problem consists in determining an inverse function $f=F^{-1}$ that gives us the information on r and n (the output data).

- The training data

We have calculated a set of vectors x containing the 51 elements representing the intensities obtained at λ=632.8 nm, by varying the parameters r and m: these vectors have been used as input quantities for training the network. The radius of the particles has been varied in the range of 50-500 nm and in Table I we report the values of the real and imaginary part of m^2 used to obtain $I(\vartheta)$.

As one can observe in **Fig.1** the input data, even in the case of sphere with the same dielectric constant, presents a large spread of the numeric values representing the intensities (y axis) so it has been necessary to perform normalization and scaling in the range [0,1] of all data; moreover, for a better performance of the network, the inputs calculated in the angular range 20°-170° were disordered. In **Fig. 1a** we plot the same data represented in fig1 after the procedure of normalization and mixing.

- The training algorithm

We have employed a feed-forward neural network, also called perceptron. The type of training algorithm employed that yield the best results is based on the Levenberg-Marquardt method. This algorithm gives fast convergent results even if it requires a greater amount of computer memory. To take advantage of the neural network's nonlinear approximation capabilities requires, in addition to an input and an output layer, one hidden or intermediate layer. The activation functions used for the hidden layer are the tansig function and for the output layer the purelin function. Moreover, the exact size of the hidden layer has to be determined empirically.

- Conclusion

As shown in **Fig 2,** the most successful network configuration found in this study uses 51 inputs (the intensities), 10 hidden neurons with 3 outputs (r, real and imaginary part of m^2).

As a measure of goodness, we have calculated the correlation coefficient defined as follows:

$$R=\frac{\sum_j (x_{1j}-\bar{x}_1)(x_{2j}-\bar{x}_2)}{\sqrt{\sum_j (x_{1j}-\bar{x}_1)^2 \sum_j (x_{2j}-\bar{x}_2)^2}}$$

where x_1 and x_2 are two observed quantities and $\bar{x}_i$ is the mean of the observed value for the i-type sample.

In **Figs 3-6** we collected the relevant results obtained by means the sotfware package MATLAB implemented on a Pentium III with 256 MB of RAM. In fig.4, 5 and 6 we can observe that after 1000 training cycles (epochs) the retrieved coefficients (red curves) are in a quite good agreement with the target parameters (blue curves). Even if the better agreement regards the radius that gives a correlation coefficient of 0.99574 (see table II), we can assess that the performance of the network is still good also for the dielectric constants. It is useful to highlight the goodness of the index of performance of the network given by the small value of mean squared error (see Table II).

Re(m^2)	Im(m^2)
1.857769	0
1.863225	0
1.865956	0
2.197213	0
2.2801	0
2.3010707	0.0003033
2.3104	0
2.528100	0
2.592084	0.012880
2.592116	0.01288
2.702736	0
2.94499	0.001420
3.5721	0
3.8479	1.56
4.149050	3.510516
5.8564	0

TABLE 1

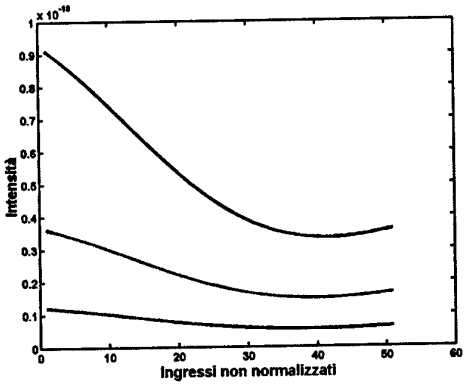

Fig. 1 Pattern of a set of three non normalized input data

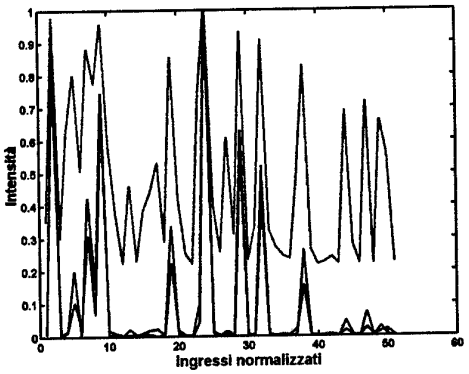

Fig. 1a Pattern of the mixed and normalized input data represented in fig 1.

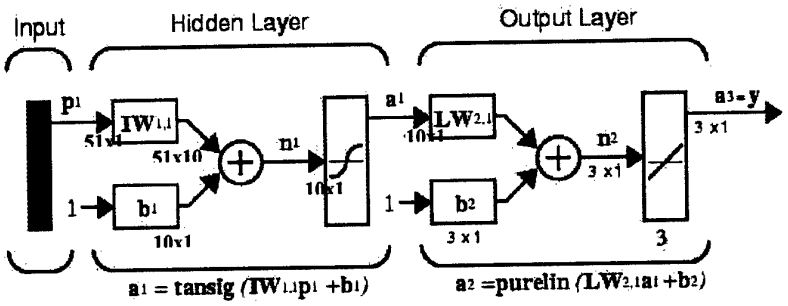

Fig 2 – Scheme of the Neural Network implemented with the software package MATLAB

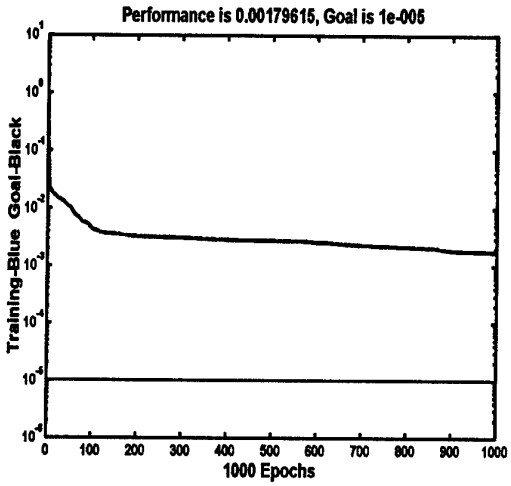

Fig. 3 Development of the rms error for training and test data set during neural-network training

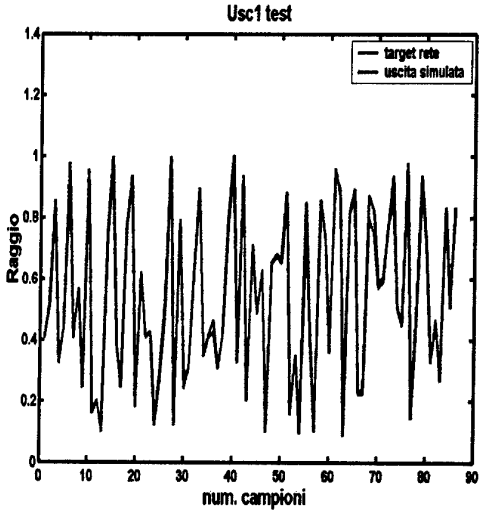

Fig. 4 Comparison between the target values of the radius (blue curve) and simulated ones, output of the neural network (red curve).

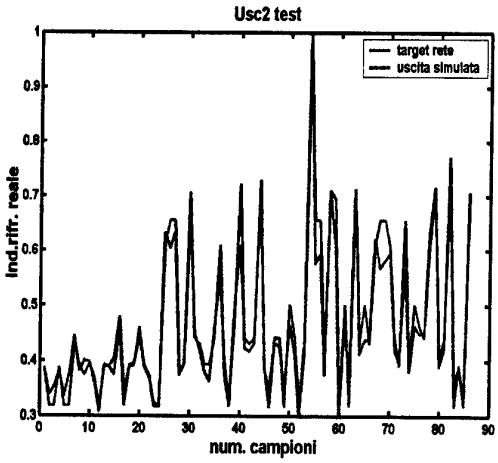

Fig. 5 The same of fig 3 but for the real part of dilectric constant.

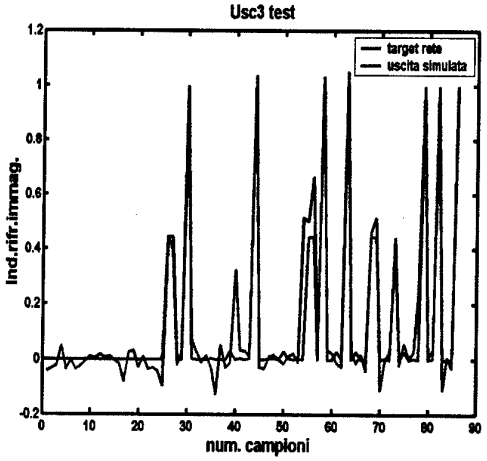

Fig. 6 The same of fig 3 but for the imaginary part of dielectric constant.

	Radius	$Re(n^2)$	$Im(n^2)$
Correlation coefficient	0,99574	0,9690	0,95682

Efficient Light Scattering Calculation for Aggregates of Large Spheres

It is well known that a possible means for determining shape and structure information about airborne microparticles is to investigate the angular scattering pattern that is done usually in only one angular dimension (ϑ).

However, as the elastic scattered angular intensity distribution from nonspherical particles has an azimuthal (φ) as well as a polar (ϑ) dependence, observation of the two-dimensional angular optical scattering (TAOS) is a more useful tool for determining the shape and the structure of microparticle aggregates. Recently, Holler et al. (1) have devised an experimental setup that is able to illuminate a single scatterer and to measure its TAOS for scattering angles that go from forward to backward direction. In view of the capability of this new experimental device, we discuss how and to what extent the computational effort can be reduced still preserving the quantitative features of the signature of a sample aggregate. As we are not interested to use orientational averaging procedure, we perform all the calculation for a microparticle aggregate in the framework of the E-scheme that prevents us to obtain the transition matrix that requires a high computational effort.

The description of E-scheme, the results of the calculation and the comments, also presented at the Annual Scientific Conf. On Obscuration ad Aerosol Res. (Abardeen Md,USA, June 2001), are widely discussed in the following paper that will be published in Applied Optics.

Efficient Light Scattering Calculations for Aggregates of Large Spheres

Rosalba Saija, Maria Antonia Iatì, Paolo Denti, Ferdinando Borghese, Arianna Giusto

Università di Messina, Dipartimento di Fisica della Materia e Tecnologie Fisiche Avanzate, and Istituto Nazionale per la Fisica della Materia, Unità di Messina, Salita Sperone, 31 — 98166 Messina, Italy

O. I. Sindoni

Edgewood Chemical Bacteriological Center, Aberdeen P. G., Gunpowder Branch, MD 21010, USA

The calculation of the scattering pattern from aggregates of spheres through the T-matrix approach yields high precision results but at an high computational cost specially when the aggregate concerned is big or is composed of big-sized spheres. With reference to a specific but representative aggregate, we discuss how and to what extent the computational effort can be reduced still preserving the qualitative features of the signature of the aggregate concerned. © 2002 Optical Society of America

OCIS codes: 000.0000, 999.9999.

1. Introduction

The scattering properties of spherical particles, both homogeneous and radially non-homogeneous, can be easily and accurately calculated through Mie theory[1] or one of its extensions[2] over a wide range of radii and wavelengths. The theoretical predictions are in both qualitative and quantitative agreement with the observations provided the experimental setup and measured parameters faithfully reproduce the assumed theoretical model (actual sphericity of the scatterer, dielectric constant, scattering angle, etc...).[3]

The situation is quite different when the scatterer is not spherically symmetric; in that case the calculation of the scattering properties (scattering amplitude, scattering and extinction cross sections, scattered intensity) with an accuracy of 3 or 4 significant digits, may become quite a cumbersome task, particularly as the size of the scatterer gets bigger and bigger. Performing calculations to so high an accuracy, however, makes sense when one is interested in the properties of just one well characterized particle but, when the theoretical predictions are to be compared with the experimental data from an assembly of scatterers, such a computational effort may be pointless. Consider, for instance, a sample made of a dispersion of non spherical particles: as a rule, the component particles are not identical nor equioriented so that

many parameters are required to fully characterize the dispersion. In view of the unavoidable imprecision in the determination of each of the parameters involved in the description of the sample, a complete characterization of the scatterers is not needed: a model reproducing the overall shape and symmetry of the scatterer may be a good one to perform the calculations. Moreover, the effort devoted to the calculation of the scattering properties of individual particles can be somewhat reduced. Of course the question arises: what degree of precision is reasonable to pursue in the calculations to get a satisfactory description of the scattering properties of the particles and what is the most suitable computational technique to achieve this precision? An accuracy within e.g. 10% could be enough to give a good qualitative description of the individual scatterers, to be integrated in the overall description of the dispersion.

Assuming that a model for the particles has been chosen, one has still to choose the most suitable computational technique to get a satisfactory description of their scattering properties, as several computational methods imply an intrinsic accuracy that stems from the assumptions on which they are based. In this respect, methods based on series expansions are able to give results whose accuracy can be graduated according to the need: in fact, we recall that Mie theory itself is just a series expansion method. Let us consider also the problem of scattering from a particle that actually is or can be modeled as an aggregate of spherical scatterers. By expanding the field in a series of vector multipole fields one is able to get the transition matrix and the scattering amplitude of the whole aggregate within an approximation that depends only on the maximum order of the multipole fields that are included into the expansion. This is a useful circumstance because, when the number of the spheres in the aggregate is large or when the individual size of the component spheres is big the computational effort grows more and more heavy, so that, determining the minimal acceptable accuracy of the results becomes an important issue.

In order to give a quantitative content to the above considerations we devote this paper to the determination of the minimal acceptable accuracy of scattering calculation for a big cluster of spheres through the method of expansion that we mentioned above. To this end, we chose to deal with the same model scatterer that has already been considered by Holler et al.[4] We stress, however, that our purpose is not to compare our calculations with the predictions in Ref.4 or with the experimental data; our purpose is instead to investigate through the specific case we deal with how and to what extent computational efforts can be reduced still getting a reliable qualitative description of the scattering pattern. To perform our task a two-step calculation proved to be more viable than a single-step one. Accordingly, first we reduce the geometrical dimensions of the scatterer leaving unchanged everything else; doing this, on one hand drastically reduces the difficulties connected with the computation and the time required to perform it, and on the other hand allows us to work out the conditions that ensure the stability of the results from a qualitative point of view. In other words we want to determine the conditions under which the calculated scattering pattern qualitatively reproduce the exact one in the sense that it reproduces the scattering signature of the individual particle. In the second step, we consider the model scatterer with its full dimensions and we apply the already tested stability criteria so to get a scattering pattern whose validity, at least from a qualitative point

of view, is reasonably ensured.

Section 2 gives a brief description of the theoretical approach, devoting particular attention to the aspects regarding the convergence and the stability of the results. Section 3 is devoted to the presentation and discussion of the results and finally in section 4 we draw a few conclusive remarks.

2. Scattering by clusters of spheres. Theory

In order to fix the notation, let us state that the polarization of the incident and of the scattered field is described with reference to two pairs of mutually orthogonal unit vectors, $\hat{\mathbf{u}}_{I\eta}$ and $\hat{\mathbf{u}}_{S\eta}$, with $\eta = 1, 2$, such that

$$\hat{\mathbf{u}}_{I1} \times \hat{\mathbf{u}}_{I2} = \hat{\mathbf{k}}_I, \quad \hat{\mathbf{u}}_{S1} \times \hat{\mathbf{u}}_{S2} = \hat{\mathbf{k}}_S.$$

In this paper we choose

$$\hat{\mathbf{u}}_{I1} = \hat{\boldsymbol{\vartheta}}_I, \quad \hat{\mathbf{u}}_{I2} = \hat{\boldsymbol{\varphi}}_I$$

and

$$\hat{\mathbf{u}}_{S1} = \hat{\boldsymbol{\vartheta}}_S, \quad \hat{\mathbf{u}}_{S2} = \hat{\boldsymbol{\varphi}}_S,$$

where $\hat{\boldsymbol{\vartheta}}_I$, $\hat{\boldsymbol{\varphi}}_I$, $\hat{\boldsymbol{\vartheta}}_S$, $\hat{\boldsymbol{\varphi}}_S$ are unit vectors along the meridians and the parallels of the unit spherical surface with center within the scattering particle at the points $\hat{\mathbf{r}} = \hat{\mathbf{k}}_I$ and $\hat{\mathbf{r}} = \hat{\mathbf{k}}_S$, respectively.[5] Hereafter we denote an incident field polarized along $\hat{\mathbf{u}}_{I\eta}$ as $\mathbf{E}_{I\eta}$ and the corresponding scattered field as $\mathbf{E}_{S\eta}$.

Let us consider a cluster of spheres, numbered by the index α, of radius ρ_α and refractive index n_α, whose centers lie at $\mathbf{R}_\alpha$, embedded into a non-absorptive medium of refractive index n. Neither the radii nor the refractive indexes of the component spheres need to be equal to each other. The electromagnetic field is expanded in terms either of the vector multipole fields $\mathbf{J}_{lm}^{(p)}$, with

$$\mathbf{J}_{lm}^{(1)}(\mathbf{r}, K) = j_l(Kr)\mathbf{X}_{lm}(\hat{\mathbf{r}}), \quad \mathbf{J}_{lm}^{(2)}(\mathbf{r}, K) = \frac{1}{K}\nabla \times \mathbf{J}_{lm}^{(1)}(\mathbf{r}, K)$$

that are regular at the origin, or of the multipole fields $\mathbf{H}_{lm}^{(p)}$ that are identical to the $\mathbf{J}$ multipole fields except for the substitution of the Hankel functions of the first kind h_l in place of the Bessel functions j_l and thus satisfy the radiation condition at infinity. In the preceding equations the vector functions $\mathbf{X}_{lm}$ are vector spherical harmonics[8] and the superscript p is a parity index that distinguishes the magnetic multipoles ($p = 1$) from the electric ones ($p = 2$). We assume that all the fields depend on time through the factor $\exp[-i\omega t]$, that is omitted throughout, and define the propagation constant in vacuo $k = \omega/c$.

The incident field is assumed to be a polarized plane wave and is expanded as

$$\mathbf{E}_{I\eta}(\mathbf{r}) = E_0 \sum_{plm} \mathbf{J}_{lm}^{(p)}(\mathbf{r}, nk) W_{I\eta lm}^{(p)},$$

where $W^{(p)}_{I\eta lm} = W^{(p)}_{lm}(\hat{\mathbf{u}}_{I\eta}, \hat{\mathbf{k}}_I)$ with

$$W^{(p)}_{lm}(\hat{\mathbf{e}}, \hat{\mathbf{k}}) = 4\pi i^{p+l-1} \hat{\mathbf{e}} \cdot \mathbf{Z}^{(p)*}_{lm}(\hat{\mathbf{k}}),$$

where we define the transverse harmonics

$$\mathbf{Z}^{(1)}_{lm}(\hat{\mathbf{k}}) = \mathbf{X}_{lm}(\hat{\mathbf{k}}), \quad \mathbf{Z}^{(2)}_{lm}(\hat{\mathbf{k}}) = \mathbf{X}_{lm}(\hat{\mathbf{k}}) \times \hat{\mathbf{k}}.$$

The field scattered by the whole cluster is written as the superposition of the fields scattered by the single spheres

$$\mathbf{E}_{S\eta} = E_0 \sum_{\alpha} \sum_{plm} \mathbf{H}^{(p)}_{lm}(\mathbf{r}_\alpha, nk) \mathcal{A}^{(p)}_{\eta\alpha lm}, \tag{1}$$

where $\mathbf{r}_\alpha = \mathbf{r} - \mathbf{R}_\alpha$, whereas the field within the α-th sphere is expanded as

$$\mathbf{E}_{T\eta\alpha} = E_0 \sum_{plm} \mathbf{J}^{(p)}_{lm}(\mathbf{r}_\alpha, n_\alpha k) \mathcal{C}^{(p)}_{\eta\alpha lm}. \tag{2}$$

The amplitudes $\mathcal{A}^{(p)}_{\eta\alpha lm}$ and $\mathcal{C}^{(p)}_{\eta\alpha lm}$ in Eqs.(1) and (2) are determined by the customary boundary conditions across the surface of each sphere in the cluster, and their knowledge totally solves the problem of the dependent scattering from the aggregate; in fact, for each value of α, the $\mathcal{A}^{(p)}_{\eta\alpha lm}$ describe the scattering by the α-th sphere, due to the incident plane wave and to the waves previously scattered by all the other spheres in the aggregate. Anyway, using the procedure that is fully described e.g. in Ref. 9, the amplitudes $\mathcal{A}^{(p)}_{\eta\alpha lm}$ turn out to be the solution to the system of linear non-homogeneous equations

$$\sum_{\alpha'} \sum_{p'l'm'} \mathcal{M}^{(pp')}_{\alpha lm\alpha' l' m'} \mathcal{A}^{(p')}_{\eta\alpha' l' m'} = -\mathcal{W}^{(p)}_{\eta\alpha lm}, \tag{3}$$

where we define the *shifted* amplitudes of the incident field

$$\mathcal{W}^{(p)}_{\eta\alpha lm} = \sum_{p'l'm'} \mathcal{J}^{(pp')}_{\alpha lm0l'm'} W^{(p')}_{I\eta l'm'}. \tag{4}$$

The quantities $\mathcal{J}^{(pp')}_{\alpha lm0l'm'}$ are the elements of the matrix that, according to the addition theorem for multipole fields,[6] translates these fields from the origin of the coordinates O at $\mathbf{R}_0 = 0$ to $\mathbf{R}_\alpha$, i.e. to the center of the α-th sphere, and

$$\mathcal{M}^{(pp')}_{\alpha lm\alpha' l' m'} = \left(R^{(p)}_{\alpha l}\right)^{-1} \delta_{\alpha\alpha'} \delta_{pp'} \delta_{ll'} \delta_{mm'} + \mathcal{H}^{(pp')}_{\alpha lm\alpha' l' m'}. \tag{5}$$

In Eq. (5) the quantities $R^{(1)}_{\alpha l}$ and $R^{(2)}_{\alpha l}$ are the elements of the transition matrix for the α-th sphere and, except for a sign, coincide with the customary Mie coefficients b_l and a_l, respectively; the quantities $\mathcal{H}^{(pp')}_{\alpha lm\alpha' l' m'}$, whose explicit expression is given in Ref.7, come from the addition theorem of Ref. 6 take account of the multiple scattering processes that occur among the spheres in the aggregate.

A. *T-scheme*

In principle, the amplitudes $\mathcal{A}^{(p')}_{\eta\alpha'l'm'}$ contain all the information on the scattering properties of the cluster concerned. In fact, we will now discuss two schemes for the extraction of the relevant information from the solution to system (3), the choice being dictated by the kind of information one is interested in. The first scheme, that we summarize in the present subsection, is the most complete as it produces the T-matrix of the scatterer. To this end, letting M be the matrix whose elements are given by Eq.(5), we recall that the formal solution to system (3),

$$\mathcal{A}^{(p)}_{\eta\alpha lm} = -\sum_{p'l'm'} \left[\mathsf{M}^{-1}\right]^{(pp')}_{\alpha lm\alpha'l'm'} \mathcal{W}^{(p')}_{\eta\alpha'l'm'}, \tag{6}$$

resembles the definition of the T-matrix.[10] Nevertheless, M^{-1} does not coincide with the T-matrix of the aggregate because, according to Ref. 10, the transition matrix relates the multipole amplitudes of the incident field to those of the field scattered by the whole object, whereas Eq. (6) relates the amplitudes of the incident field to those of the fields scattered by each sphere in the aggregate. Nevertheless, the addition theorem of Ref.6 allows us to write the scattered field in terms of multipole fields with origin at O as

$$\mathbf{E}_{S\eta} = E_0 \sum_{plm} \sum_{\alpha'} \sum_{p'l'm'} \mathbf{H}^{(p)}_{lm}(\mathbf{r}, nk) \mathcal{J}^{(pp')}_{0lm\alpha'l'm'} \mathcal{A}^{(p')}_{\eta\alpha'l'm'}$$

and consequently to write the amplitudes of the field scattered by the whole aggregate as

$$A^{(p)}_{\eta'lm} = \sum_{\alpha'} \sum_{p'l'm'} \mathcal{J}^{(pp')}_{0lm\alpha'l'm'} \mathcal{A}^{(p')}_{\eta'\alpha'l'm'}, \tag{7}$$

where the quantities $\mathcal{J}^{(pp')}_{0lm\alpha'l'm'}$, whose explicit expression is given in Ref.7, are the elements of the matrix that translates the origin of the **H**-multipole fields from $\mathbf{R}_{\alpha'}$ to the origin of the coordinates at O.

At this stage the expression for the amplitudes $\mathcal{A}^{(p')}_{\eta'\alpha'l'm'}$ given by Eq. (6) can be substituted into Eq. (7) that consequently reads

$$A^{(p)}_{\eta'lm} = \sum_{p'l'm'} \mathcal{S}^{(pp')}_{lml'm'} W^{(p')}_{I\eta'l'm'},$$

where the elements of the true T-matrix of the aggregate are

$$\mathcal{S}^{(pp')}_{lml'm'} = -\sum_{\alpha\alpha'} \sum_{qLM} \sum_{q'L'M'} \mathcal{J}^{(pq)}_{0lm\alpha LM} \left[\mathsf{M}^{-1}\right]^{(qq')}_{\alpha LM\alpha'L'M'} \mathcal{J}^{(q'p')}_{\alpha'L'M'0l'm'}. \tag{8}$$

The elements $\mathcal{S}^{(pp')}_{lml'm'}$ account for all the scattering properties of the cluster. In fact, in the far zone the scattered field assumes the asymptotic form

$$\mathbf{E}_{S\eta} = E_0 \frac{\exp(inkr)}{r} \mathbf{f}_\eta(\hat{\mathbf{k}}_S, \hat{\mathbf{k}}_I) = \frac{E_0}{nk} \frac{\exp(inkr)}{r} \sum_{plm} (-i)^{l+p} \mathbf{Z}^{(p)}_{lm}(\hat{\mathbf{k}}_S) A^{(p)}_{\eta lm},$$

where $\mathbf{f}_\eta$ is the scattering amplitude[8] and Eq. (7) has been used. Therefore the component of the scattered field that is polarized along $\hat{\mathbf{u}}_{S\eta}$ reads

$$\mathbf{E}_{S\eta'} \cdot \hat{\mathbf{u}}_{S\eta} = E_0 \frac{\exp ikr}{r} f_{\eta\eta'}$$

with

$$f_{\eta\eta'} = -\frac{i}{4\pi nk} \sum_{plm} \sum_{p'l'm'} W^{(p)*}_{S\eta lm} \mathcal{S}^{(pp')}_{lml'm'} W^{(p')}_{I\eta'l'm'} \tag{9}$$

and $W^{(p)}_{S\eta lm} = W^{(p)}_{lm}(\hat{\mathbf{u}}_{S\eta}, \hat{\mathbf{k}}_S)$. As a consequence, the scattered intensity, both co-polarized and cross-polarized, turns out to be

$$I_{\eta\eta'} = \frac{|E_0|^2}{r^2} |f_{\eta\eta'}(\hat{\mathbf{k}}_S, \hat{\mathbf{k}}_I)|^2.$$

Hereafter we will refer to the procedure outlined above as the T-scheme.

B. E-scheme

We now come to describe an alternative scheme, the E-scheme, that, in some instances, has useful computational advantages. We start remarking that, when Eq. (8) is substituted into Eq. (9) to get the components of the scattering amplitude, the resulting expression contains the terms

$$\sum_{plm} W^{(p)*}_{S\eta lm} \mathcal{J}^{(pq)}_{0lm\alpha LM} \qquad \text{and} \qquad \sum_{p'l'm'} \mathcal{J}^{(q'p')}_{\alpha'L'M'0l'm'} W^{(p')}_{I\eta'l'm'}$$

that can be somewhat simplified as follows. Since $\mathbf{r} = \mathbf{R}_\alpha + \mathbf{r}_\alpha$,

$$\exp[i\mathbf{k}_I \cdot \mathbf{r}] = \exp[i\mathbf{k}_I \cdot \mathbf{R}_\alpha] \exp[i\mathbf{k}_I \cdot \mathbf{r}_\alpha] \, .$$

Therefore, by expanding $\hat{\mathbf{u}}_{I\eta} \exp[i\mathbf{k}_I \cdot \mathbf{r}]$ and $\hat{\mathbf{u}}_{I\eta} \exp[i\mathbf{k}_I \cdot \mathbf{r}_\alpha]$ we get

$$\mathcal{W}^{(p)}_{\eta\alpha lm} = \exp[i\mathbf{k}_I \cdot \mathbf{R}_\alpha] W^{(p)}_{I\eta lm}.$$

Comparison of the latter equation with Eq. (4) yields

$$\sum_{p'l'm'} \mathcal{J}^{(pp')}_{\alpha lm0l'm'} W^{(p')}_{I\eta l'm'} = \exp[i\mathbf{k}_I \cdot \mathbf{R}_\alpha] W^{(p)}_{I\eta lm}. \tag{10}$$

Substitution into Eq.(10) of $\hat{\mathbf{u}}_{S\eta}$ in place of $\hat{\mathbf{u}}_{I\eta}$ and $\mathbf{k}_S$ in place of $\mathbf{k}_I$ and complex conjugation then yields

$$\sum_{p'l'm'} \mathcal{J}^{(pp')*}_{\alpha lm0l'm'} W^{(p')*}_{S\eta l'm'} = \exp[-i\mathbf{k}_S \cdot \mathbf{R}_\alpha] W^{(p)*}_{S\eta lm}.$$

Now, on account that the refractive index n is real, we get[11]

$$\mathcal{J}^{(pp')*}_{\alpha lm0l'm'} = \mathcal{J}^{(p'p)}_{0l'm'\alpha lm},$$

so that

$$\sum_{p'l'm'} W^{(p')*}_{S\eta l'm'} \mathcal{J}^{(p'p)}_{0l'm'\alpha lm} = \exp[-i\mathbf{k}_S \cdot \mathbf{R}_\alpha] W^{(p)*}_{S\eta lm}. \tag{11}$$

Using Eqs.(10) and (11), $f_{\eta\eta'}$ takes on the final form

$$f_{\eta\eta'} = \frac{i}{4\pi nk} \sum_{pLM} \sum_{p'L'M'} \sum_{\alpha\alpha'} W^{(p)*}_{S\eta LM} \exp[-i\mathbf{k}_S \cdot \mathbf{R}_\alpha] \times [\mathsf{M}^{-1}]^{(pp')}_{\alpha LM\alpha' L'M'} \exp[i\mathbf{k}_I \cdot \mathbf{R}_{\alpha'}] W^{(p')}_{I\eta' L'M'}.$$

We stress that unlike the approximate scheme of Xu[12] to get the expression of the scatterd field in the far zone, the E-scheme is exact as it implies no further approximation beyond the customary truncation of the multipole expansions. We tested the reliability of this scheme by using it extensively to compare our theoretical predictions[13] with the experimental data of Schuerman and Wang from well characterized clusters in fixed orientation.[14,15]

C. Convergence

According to T-scheme, calculation of the transition matrix of a cluster requires inverting the matrix M whose order is, in principle, infinite. Naturally, system (3) must be truncated to some finite order by including in Eq.(8) terms up to order L_M, that is the maximum value both for L and L', chosen so as to ensure the required accuracy of the transition matrix elements. For a cluster of N spheres this implies to solve a system of order $D_M = 2NL_M(L_M + 2)$ that may grow rather big. Actually, the inversion of the matrix M is responsible for most of the time required for the calculation; this time scales, in fact, as D_M^3. According to the considerations in Section 1, L_M must be so chosen that using an increased L_M the pattern of the scattered intensity no more undergoes any qualitative changes. Choosing the least adequate L_M is thus decisive: on account of the definition of D_M, computation time increases as L_M^6 and storage as L_M^4. Therefore, using too big an L_M would require a computer time that is definitely longer than a real-time calculation that may be required e.g. for medical or meteorological applications. It may be worth remarking that L_M could take a different value for each of the spherical components of the cluster we deal with: in other words, there is no reason why l in Eqs.(1) and (2) should not assume a maximum value that depends on α. As a noticeable consequence, D_M could be somewhat reduced. This is in connection with the obvious remark that the spherical components, according to their own scattering power, may give considerably different contributions to the scattering from the cluster as a whole. Such a refinement in assigning L_M, however, is of no use when the scattering powers of the individual components are similar and when one deals with compact structures. Since in Sect.3 we will deal just with a cluster of this kind, we will assign only one value of L_M to be applied to each of the spheres composing the cluster.

At this stage, it may be useful to make a few quantitative considerations about choosing L_M for exact convergence, i.e. convergence to $\approx$ 3–4 significant digits. For

a dielectric sphere with radius b_s we have to choose $L_M > kb_s + m_s$; when we deal with a cluster of spheres, we get the exact description of the scattering problem considering $L_M > kb_c + m_c$, where b_c is the radius of the smallest sphere including the whole aggregate. The numbers m_s and m_c are positive integers that depend on the refractive indexes; in general, if kb_s and kb_c are large $m_s \ll kb_s$ and $m_c \ll kb_c$. Nevertheless, in the next section, we will show that, in order to give a good qualitative description of the scattering properties of the aggregate we consider it is sufficient to use a value for L_M that would rather be appropriate to the exact description of the scattering from a single sphere of the aggregate. The validity of our choice for L_M will be checked by looking wether or not the scattering properties of the whole aggregate, thus calculated, will still keep their qualitative features with increasing value of L_M.

Finally, let us stress that the T-scheme and the E-scheme are not the only possible ones to describe scattering from aggregated spheres. In fact, schemes have been devised that do not require direct inversion of matrix M as well as schemes in which the averaging and inversion are integrated in a single computational procedure.[16,17] As all these alternative schemes are aimed at minimizing the computational effort, they should be carefully considered when the main interest is the exact solution of the scattering problem.

Using the E-scheme slightly reduces the amount of calculation for a given L_M with respect to the T-scheme. In fact, the latter requires the additional calculation of the sums in the left hand side of Eqs.(10) and (11) that, in turn, is more or less onerous according to the value one assumes for l_M, the maximum l' to be included to get an accurate representation of the scattered field. E-scheme, however, prevents us to obtain the transition matrix as defined by Eq. (8) and therefore to use the orientational averaging procedure, widely described elsewhere:[18] the true transition matrix, indeed, cannot be reminiscent of information either on the excitation (through the factors $\exp[i\mathbf{k}_I \cdot \mathbf{R}_\alpha]$) or on observation (through the factors $\exp[-i\mathbf{k}_S \cdot \mathbf{R}_{\alpha'}]$). It is also to be borne in mind that once the T-scheme has been applied, another chunk of calculation is needed to perform the orientational averages. In conclusion the E-scheme is appropriate when orientational averages are not required.

3. Results and discussion

Although the cluster that we study in this paper is the same 13-spheres clusters considered by Holler et al., we stress again that our purpose is quite different, as we explained in Sect.1. The cluster of interest is composed of polystirene latex spheres with size parameter $x_s = nkb_s = 13.36$, arranged in a closely packed structure with a roundish geometry so that the overall size parameter of the whole aggregate turns out to be $x_c = nkb_c = 40$. The coordinates of the centers of the spheres are listed in Table 1; $n = 1$. According to the considerations at the end of Sect. 2 convergence to 3 decimal places would require $L_M > 40$. In Ref. 4, the calculations were performed through the recursive algorithm by Chew[19] that shares in common with our approach the fact that the only approximation lies in the choice of the value of L_M at which the multipole expansions of the electromagnetic fields are stopped. Nevertheless it appears that a generalized use of such a perturbative-iterative approach would require some

caution and artwork in its implementation. For instance, the actual achievement of convergence for a given choice of L_M should be carefully verified. On the contrary, the direct approach that we use, i.e. the E-scheme, appears to be straightforward and leaves to the researcher full control of the accuracy that can be achieved.

In the following discussion the wavevector of the incident plane wave $\hat{\mathbf{k}}_I$ has $\varphi_I = 0°$ and $\vartheta_I = 90°$, or $\vartheta_I = 45°$. The scattered intensity is calculated for $-90° \leq \vartheta_S \leq 90°$ and $0° \leq \varphi_S \leq 180°$ and is represented through contour plots. In a few cases are also reported sections of these contour plots for $\vartheta_S = 30°$ and $\vartheta_S = 90°$. Choosing $\vartheta_I = 90°$ corresponds to incident field viewing the scatterer as a highly symmetric object.

With the aim of finding a qualitative stability criterion we consider a cluster of spheres with the same geometry as the one we chose but scale down the dimensions of the component spheres to the 20 %. Since we assume that the incident field has a wavelength of 0.532 μm, the size parameter will be reduced to $x_s = 2.672$ for the single component sphere and to $x_c = 8$ for the whole cluster. We make an angular analysis of the scattered intensity in the forward scattering zone. In Fig. 1 (a), (b) and (c) we report the contour plots, calculated using the E-scheme, of the differential scattering cross section $\mathcal{I}_{\vartheta\vartheta} = |f_{\vartheta\vartheta}|^2$ for $l_M = 3, 5, 8$, respectively. The corresponding plots for $\mathcal{I}_{\varphi\varphi}$ show the same trend that we are going to discuss and are therefore not reported. Comparison of the plots (a), (b) and (c) shows that the stability is already reached for $L_M = 5$; in fact, the plots for $L_M = 5$ [Fig.1 (b)] and $L_M = 8$ [Fig.1 (c)] do not show any important difference. Note that $L_M = 5$ is, in principle, a little larger than barely sufficient to get the convergency for the component spheres. This result has been further investigated by reporting in Fig. 2 (a) the differential scattering cross section for $\vartheta_I = 90°$ and $\varphi_I = 0°$ for $L_M = 2, 3, 4, 5$; in Fig.2 (a) $\vartheta_S = 90°$ and $-90° \leq \varphi_S \leq 90°$; in Fig. 2 (b) $\vartheta_S = 30°$ and $-90° \leq \varphi_S \leq 90°$. The plots in both Fig.2 (a) and Fig.2 (b) show that the changes undergone by the intensity profiles for $L_M \geq 4$ are quite negligible. We do not report the profiles for $L_M > 5$ because, on the scale of the figure they are perfectly superposed to the profile for $L_M = 5$. We are thus led to conclude that the contour plot in Fig.1 (b), i.e. for $L_M = 5$, gives a good description of the actual scattered intensity and that $L_M = 4$ is sufficient to get an acceptable qualitative description.

As regards the behavior of the T-scheme, we found, as expected, that $l_M > L_M$ is required to get full convergence in the sums in Eq.(10) and (11) so as to reproduce the results obtained in the E-scheme for the same value of L_M. In practice, we report in Fig.3 the intensity profiles of Fig.2 (a), calculated with $L_M = 4$ both in the E and T-scheme and, in the latter case, for increasing values of l_M. The curves in Fig.3 show at once that, although $l_M = 8$ is quite acceptable, and that $l_M = 10$ is even better, the results of the E and T-scheme become indistinguishable on the scale of the figure for $l_M = 12$. Such a perfect convergence is unnecessary, however, as it would yield the perfect reproduction of the results of the E-scheme for $L_M = 4$, that are in their nature qualitative results. Thus, one could choose for l_M the least value that would not disrupt the qualitative behavior of the scattering pattern: according to Fig.3, $l_M = 8$ is a fair choice. This is yet a large value so that there is a cost, in particular when averaging over the orientation of the scatterer is in order. Anyway, we can conclude

that using the E-scheme, a good stability criterion requires using a value of L_M just a little bigger than necessary to get the convergency for the component spheres.

In order to test the stability criterion just found, we calculate, using the E-scheme, the scattering pattern of the cluster considered with its real dimensions: in this respect we recall that now $x_s = 13.36$. The results are reported for $\vartheta_I = 90°$ and $\varphi_I = 0°$ in Fig.4 for $L_M = 13$ in (a) and for $L_M = 15$ in (b); the pattern for $\vartheta_I = 45°$ and $\varphi_I = 0°$ is reported in Fig.5 for $L_M = 13$ in (a) and for $L_M = 15$ in (b). Even a cursory examination of the patterns in Figs.4 and 5 shows that the stability criterion is effective in yielding patterns that give an acceptable qualitative description of the scattering properties of the cluster at hand. In fact, when L_M is increased from 13 to 15 the changes undergone by the patterns are small on the scale of the figure. Even in this case, however, the numerical output shows that an accuracy to 3 decimal places has not yet been achieved.

4. Conclusions

At first glance, the stability criterion that we found in Sect. 3 may be rather surprising. In fact, the calculations in Sect. 3 support the conclusion that by chosing an l_M barely sufficient to ensure the convergence of the field scattered by the component spheres, one also achieves an acceptable stability of the scattering pattern from the whole cluster. Nevertheless, let us recall that the pattern from the cluster differ from that of the independent spheres because of the coupling effected by the multipole translation matrix elements $\mathcal{H}^{(pp')}_{\alpha lm\alpha' l' m'}$ in Eq. (5). These quantities, as appears from their explicit expression in Ref. 7, heavily depend on the distance between the centers of the spheres and are bound to be small, even for contacting spheres, when the radius of the latter is large. Of course, the translation matrix elements are even smaller for noncontacting spheres. As a result, in spite of the coupling, the scattering pattern from a cluster of big spheres is governed by the scattering power of the spherical components, that is given by the Mie coefficients $R^{(p)}_{\alpha l}$. Of course, the criterion that we found in Sect. 3, may not be strictly valid for a cluster whose spherical components have strongly different scatting power. In such a case a more detailed analysis is in order by chosing, as we suggested in Sect. 2, a different l_M for each sphere.

Anyway, the calculations that we presented in Sect. 3 support our considerations in Sect. 1 on the accuracy that is reasonable to pursue when calculating the optical properties of model particles. In fact, the particles that are produced in actual experiments are often not well characterized whereas the mathematical techniques may give results that are strongly dependent on the exact geometry, size and orientation of the particles concerned. This is just the problem that has been faced by Mishchenko and Mackowski in comparing their theoretical predictions with the experimental data from bispheres.[20,21] These authors state that they were forced to repeat their calculations several times changing the size of the particles in order to get results reasonably resembling the experimental findings. It is evident that the computational effort in the case of bispheres is much lighter than in the case of the 13-sphere cluster we deal with in this paper.[22] Therefore, using the stability criterion we established in Sect 3, possibly in the framework of the E-scheme, will save a lot of calculations,

still reproducing the main features of the signature of the particle concerned. This, in turn, would make viable repeating of the calculations in order to get the patterns that better resemble the experimental data.

Acknowledgements

The authors gratefully acknowledge the financial support of the U.S. Army European Reserch Office through Contract N68171-01-M-5907.

References

1. H. C. van de Hulst, *Light scattering by small particles*, (Wiley, New York, 1957)
2. P. J. Wyatt, "Scattering of electromagnetic plane waves from inhomogeneous spherically symmetric objects," Phys. Rev. B **127**, 1837–1843 (1962).
3. M. I. Mishchenko, W. J. Winscombe, J. H. Hovenier, L. D. Travis: 'Overview of scattering by nonspherical particles'. In: *Light Scattering by Nonspherical Particles*, ed. by M. I. Mishchenko, J. W. Hovenier, L. D. Travis (Academic Press, New York, 2000), pp. 30–59.
4. S. Holler, B. Stout, Y. Pan, J. R. Bottiger, R. K. Chang and G. Videen, "Observations and calculations of light scattering from clusters of spheres," Appl. Opt. **39**, 6873–6887 (2000)
5. M. I. Mishchenko, J. W. Hovenier and L. D. Travis: 'Concepts, terms, notation'. In: *Light Scattering by Nonspherical Particles*, ed. by M. I. Mishchenko, J. W. Hovenier, L. D. Travis (Academic Press, New York, 2000), pp. 3–25
6. F. Borghese, P. Denti, G. Toscano and O. I. Sindoni, "An addition theorem for vector Helmholtz harmonics," J. Math. Phys. **21**, 2754–2755 (1980)
7. F. Borghese, P. Denti and R. Saija, "Optical properties of spheres containing several spherical inclusions," Applied Optics **33**, 484–491 (1994).
8. J. D. Jackson, *Classical electrodynamics* (Wiley, New York, 1975)
9. F. Borghese, P. Denti, R. Saija, G. Toscano and O. I. Sindoni, "Multiple electromagnetic scattering from a cluster of spheres. I. Theory," Aerosol Sci. Technol. **3**, 227–235 (1984)
10. P. C. Waterman: "Symmetry, unitarity and geometry in electromagnetic scattering," Phys. Rev. D **3**, 825–839 (1971).
11. E. Fucile, F. Borghese, P. Denti, R. Saija and O. I. Sindoni, "General reflection rule for electromagnetic multipole fields on a plane interface," IEEE Trans. Antennas Propag. **AP 45**, 868–875 (1997).
12. Y.-I. Xu, "Electromagetic scattering by an aggregate of spheres: far field," Appl. Opt. **36**, 9496–9508 (1997).
13. F. Borghese, P. Denti, R. Saija and O. I. Sindoni, "Reliability of the theoretical description of electromagnetic scattering from non-spherical particles", J. Aerosol Sci. **20**, 1079–1081 (1989).
14. R. T. Wang, J. M. Greenberg and D. W. Schuerman, "Experimental results of the dependent light scattering by two spheres," Optics Lett. **11**, 543–545 (1981).
15. D. W. Schuerman, R. T. Wang: *Experimental results of multiple scattering.* Chemical Systems Laboratory Contractor Report ARCSL-CR-81003, November 1981
16. D. M. Mackowski and M. I. Mishchenko, "Calculation of the the T matrix and the scattering matrix for ensembles of spheres," J. Opt. Soc. Am. A **13**, 2266–2278 (1996).
17. M. I. Mishchenko, L. D. Travis and A. Macke, 'T-Matrix method and its applications.' In: *Light Scattering by Nonspherical Particles*, ed. by M. I. Mishchenko, J. W. Hovenier, L. D. Travis (Academic Press, New York, 2000), pp. 147–172.
18. F. Borghese, P. Denti, R. Saija, M. A. Iatì and O. I. Sindoni, "Optical properties of

a dispersion of anisotropic particles with non-randomly distributed orientations. The case of atmospheric ice crystals." J. Quant. Spectr.Radiat. Transfer **70**, 237–251 (2001)

19. W. C. Chew, *Waves and fields in inhomogeneous media*, IEEE Press Series on Electromagnetic Waves (Institute of Electrical and Electronic Engineers, Piscataway, N. J., 1990)
20. M. I. Mishchenko and D. W. Mackowski, "Electromagnetic scattering by randomly oriented bispheres: comparison of theory and experiment and benchmark calculations," J. Quant. Spectrosc. Radiat. Transfer **55**, 683–694 (1996).
21. J. R. Bottiger, E. S. Fry and R. C. Tompson, in *Light Scattering by Irregularly Shaped Particles*, D. W. Schuerman, ed. (Plenum press, New York, 1980), pp. 283–290.
22. M. I. Mishchenko, D. W. Mackowski and L. D. Travis, "Scattering of light by bispheres with touching and separated components," Appl. Opt. **34**, 4589–4599 (1995).

List of Figure Captions

Fig. 1. Contour plot of the differential scattering cross section (log scale) of the aggregate reduced to 20 % of its real size, calculated in the E-scheme. The incident field has $\vartheta_I = 90°$ and $\varphi_I = 0°$. In (a) $L_M = 3$, in (b) $L_M = 5$ and in (c) $L_M = 8$.

Fig. 2. Differential scattering cross section for the cluster reduced to 20 % of its real size, calculated in the E-scheme for $L_M = 2$ (dotted), 3 (dot-dashed), 4 (bulleted) and 5 (solid), for $\vartheta_I = 90°$ and $\varphi_I = 0°$. In (a) $\vartheta_S = 90°$; in (b) $\vartheta_S = 30°$.

Fig. 3. Comparison of the differential scattering cross section for the cluster reduced to 20 % of its real size calculated in the E-scheme for $L_M = 4$ (heavy solid line) with that yielded by the T-scheme with $L_M = 4$ and $l_M = 4$ (light solid), 6 (dot-dashed), 8 (dotted), 10 (bulleted), 12 (dashed). $\vartheta_I = 90°$, $\varphi_I = 0°$, and $\vartheta_S = 90°$. Note that the heavy solid curve and the dashed curve are almost perfectly superposed on the scale of the figure.

Fig. 4. Contour plot of the differential scattering cross section for the cluster considered with its real size calculated in the E-scheme for $\vartheta_I = 90°$ and $\varphi_I = 0°$ with $L_M = 13$ in (a) and $L_M = 15$ in (b).

Fig. 5. Contour plot of the differential scattering cross section for the cluster considered with its real size calculated in the E-scheme for $\vartheta_I = 45°$ and $\varphi_I = 0°$ with $L_M = 13$ in (a) and $L_M = 15$ in (b).

Table 1. Coordinates of the centers of the component spheres in μm. The radius and refractive index of each sphere are 1.145 μm and 1.59, respectively.

	x	y	z
1	0.00000	0.0000000	0.0000000
2	0.00000	1.9250000	-1.1890000
3	0.00000	-1.9250000	-1.1890000
4	0.00000	-1.9250000	1.1890000
5	0.00000	1.9250000	1.1890000
6	1.92500	-1.1890000	0.0000000
7	-1.92500	1.1890000	0.0000000
8	-1.92500	-1.1890000	0.0000000
9	1.92500	1.1890000	0.0000000
10	-1.18900	0.0000000	1.9250000
11	1.18900	0.0000000	1.9250000
12	1.18900	0.0000000	-1.9250000
13	-1.18900	0.0000000	-1.9250000

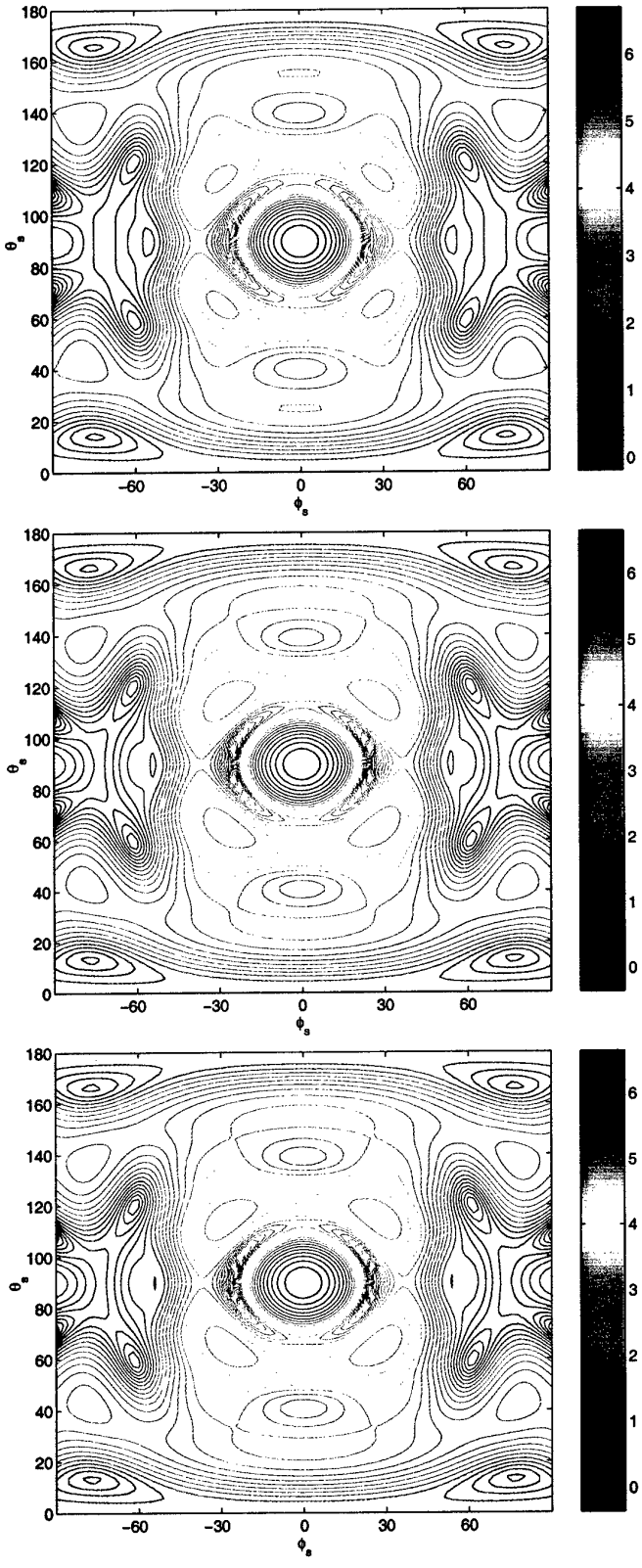
180
160
140
120
100
80
60
40
20
0
θ_s
-60
-30
0
30
60
ϕ_s
6
5
4
3
2
1
0

Fig. 1

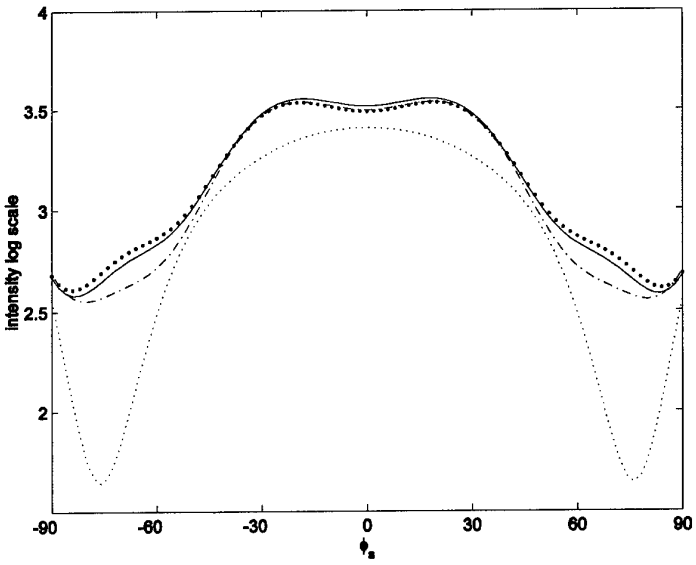
4
3.5
3
2.5
2
intensity log scale
-90
-60
-30
0
30
60
90
ϕ_s

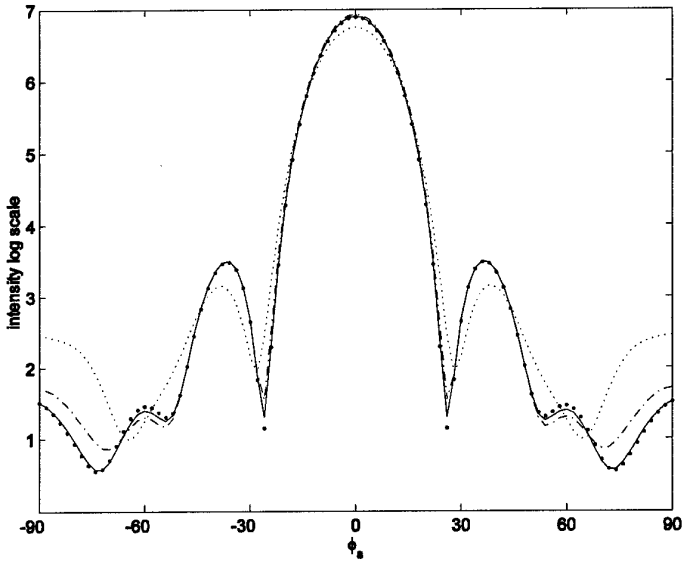
7
6
5
4
3
2
1
intensity log scale
-90
-60
-30
0
30
60
90
ϕ_s

Fig. 2

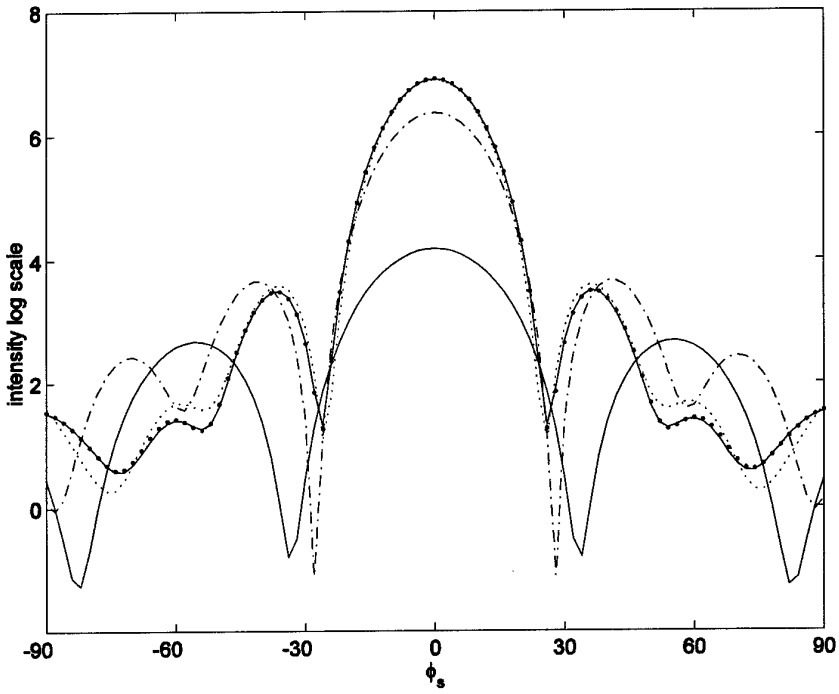

Fig. 3

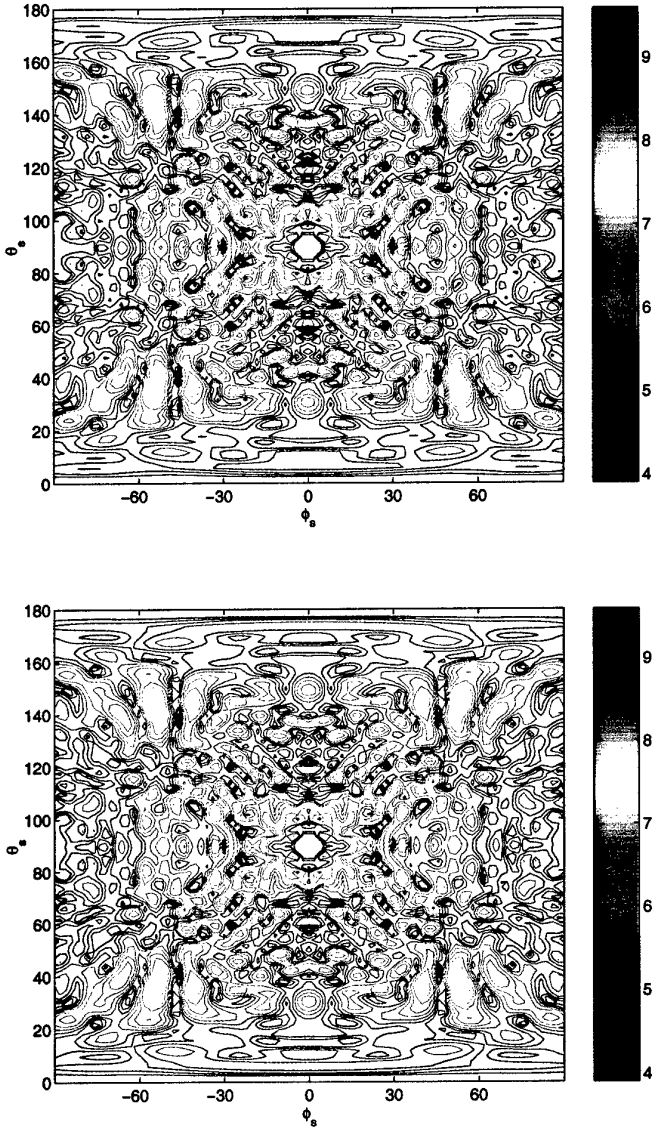

Fig. 4

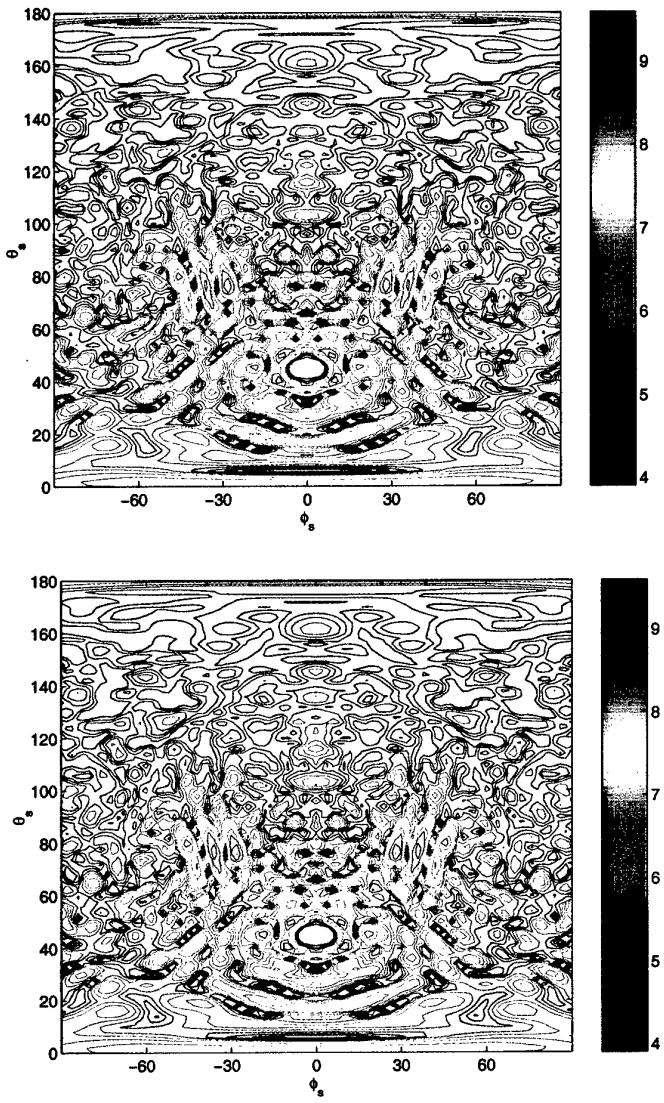

Fig. 5